SCIENCE CHINA
Information Sciences

• RESEARCH PAPER •

September 2025, Vol. 68, Iss. 9, 190304:1–190304:15
https://doi.org/10.1007/s11432-024-4511-4

Special Topic: Cohesive Clustered Satellites System for 5GA and 6G Networks

Game-theoretic clustering and scalable beamforming for multi-RIS-assisted cohesive satellite anti-jamming systems

Yucong CAO[1,2], Yifu SUN[1*], Yonggang ZHU[1], Kang AN[1] & Zhi LIN[3*]

[1]*Sixty-third Research Institute, National University of Defense Technology, Nanjing 210007, China*
[2]*College of Electronic Science and Technology, National University of Defense Technology, Changsha 410003, China*
[3]*College of Electronic Engineering, National University of Defense Technology, Hefei 230037, China*

Received 29 November 2024/Revised 16 March 2025/Accepted 6 May 2025/Published online 15 August 2025

Abstract Cohesive clustered satellites have better scalability, spatial diversity, and coverage maintainability compared with conventional single satellite platforms. However, the high complexity of massive self-organizing satellites and malicious jamming of wireless channels pose severe threats to cohesive clustered satellite systems. By utilizing game-theoretic clustering to dynamically adjust the topology of cohesive clustered satellites, combined with the use of the reconfigurable intelligent surface (RIS) for reconfiguring the jamming environment, a multi-RIS-assisted cohesive clustered satellite anti-jamming system was developed for achieving reliable communication in the presence of malicious jamming. Specifically, game-theoretic clustering forms multiple coalitions for cohesive satellites, after which the satellite RIS can constructively enhance the desired signals while destructively weakening the jamming signals within one coalition. Building upon the above system, the aim of this study is to maximize the sum rate by jointly optimizing the satellite clustering, transceiver beamforming, and phase shifts of the satellite RIS when the jammer's channel state information (CSI) is imperfect. To solve the intractable problem, the satellite clustering was first optimized by formulating a coalition formation game, where a partial optimal coalition preference order was proposed for maximizing the sum rate. Subsequently, after converting the jammer's imperfect CSI into a robust CSI by adopting the discretization method, an alternative optimization method was developed for designing the transceiver beamforming and determining the phase shifts of the satellite RIS by leveraging the zero-forcing precoder, cyclic coordinate descent optimization framework, and linear minimum-mean-square-error decoder. The results prove that the proposed game-theoretic clustering method can converge to stable coalition formation with the exact potential game. The numerical simulation results demonstrate the superiority and validity of the proposed schemes compared to existing benchmark schemes.

Keywords satellite clustering, reconfigurable intelligent surface, coalition formation game, reliable communication, anti-jamming

Citation Cao Y C, Sun Y F, Zhu Y G, et al. Game-theoretic clustering and scalable beamforming for multi-RIS-assisted cohesive satellite anti-jamming systems. Sci China Inf Sci, 2025, 68(9): 190304, https://doi.org/10.1007/s11432-024-4511-4

1 Introduction

Recently, cohesive clustered satellite communications have grown exponentially within the realms of space technology and information science [1–4]. Compared with conventional single satellites, cohesive clustered satellites have better scalability, spatial diversity, and coverage maintainability [5], thereby effectively improving the efficiency of space resource utilization. More specifically, through mutual cooperation, cohesive clustered satellites can achieve high-capacity communication with global coverage, thus enabling ubiquitous connectivity for remote areas and emergency situations.

However, the complexity of self-organizing networks between satellites increases with the number of satellites. To address this issue, satellite clustering has been adopted as a means of effectively improving the performance of cohesive satellite systems [6–12]. A satellite cluster framework that depends on the 3rd generation partnership project (3GPP) was proposed for improving the performance of cohesive satellite systems [13], where the efficiency and reliability of the entire system were enhanced by optimizing the communication protocols and standards among satellites. Moreover, a satellite routing algorithm with dynamic clustering, which effectively reduces the required storage space, was also proposed [14].

* Corresponding author (email: sunyifu_nudt@163.com, linzhi945@163.com)

Nevertheless, the above studies focused primarily on establishing clustering protocols or standards [15] that do not fully consider the topology of cohesive satellites.

Malicious jamming attacks also pose a severe threat to cohesive clustered satellites. To address this issue, various anti-jamming schemes have been widely adopted, such as the direct sequence spread spectrum and frequency-hopping [16–18]. However, both of these conventional schemes unavoidably consume additional bandwidth and energy. Although the multiple-input-multiple-output (MIMO) technique has been adopted for enhancing the desired signals and nullifying the jamming signals in low-earth-orbit (LEO) satellites [19], the implementation cost is prohibitive.

Fortunately, the reconfigurable intelligent surface (RIS), a newly emerging and innovative concept, offers an alternative scheme, in which the propagation environment can be reconfigured while maintaining low power consumption, thus boosting the desired signals and simultaneously weakening the jamming signals [20–26]. Specifically, RIS consists of massive low-cost passive reflective elements, which can dynamically change the phase shift of the desired signals, thereby improving communication performance and enhancing communication security [27]. An optimization framework was previously developed for the deployment of multi-RIS [28]. By employing graph-based network analysis, this study defines the RIS deployment problem and designs a sequential elimination method for cooperatively achieving the conflicting objectives of coverage maximization and cost minimization. Extensive simulations validated the superior cost-effectiveness of the graph-driven RIS deployment strategy compared to that of heuristic approaches. In a previous report [29], the performance of wireless energy transmission, especially the signal coverage and energy transmission efficiency in complex environments, was significantly improved by proposing and optimizing different beam-routing schemes. An innovative multi-RIS-aided downlink non-orthogonal multiple access (NOMA) framework was also designed for boosting the network throughput [30], where a sum-rate maximization problem was addressed through joint optimization of the reflection coefficients and power allocation. The simulation results demonstrated that the proposed RIS-NOMA architecture with optimized configurations attains substantial capacity improvements compared to conventional schemes.

Thus, combined with the size, power, and weight constraints of satellites, RIS can be regarded as a promising solution for enabling cohesive clustered satellite systems [31–39]. An RIS-assisted satellite network architecture was previously proposed [31], in which RIS is deployed on the satellite to act as the reflective array for achieving significant transmission gain. In another study [32], an alternating optimization scheme was proposed for optimizing the satellite RIS reflection matrix, which significantly reduced the signal quality received by the eavesdropper. Moreover, a distortion-aware beamforming design for multi-beam satellite communications with nonlinear power amplifiers was also proposed [33], achieving good performance. However, the multi-RIS-assisted cohesive cluster satellite communication system has not been studied, especially for malicious jamming with imperfect channel state information (CSI).

Motivated by the above, this study presents a novel multi-RIS-assisted cohesive clustered satellite anti-jamming (CCSAJ) system. This kind of system can guarantee the reliability of communication when encountering malicious jamming. The main contributions of this study are as follows.

(1) To the best of our knowledge, this is the first report of a novel multi-RIS-assisted CCSAJ framework that defends against jamming attacks, where the game-theoretic satellite clustering can dynamically form multiple clustered satellite coalitions, and RIS can constructively enhance the desired signals, while destructively weakening the jamming signals within one coalition. In addition, in order to achieve the maximum sum rate, a worst-case optimization problem was formulated by jointly optimizing the satellite clustering, transceiver's beamforming and phase shifts of the satellite RIS under the condition of imperfect jamming CSI.

(2) To solve the intractable optimization problem, the problem is decoupled into two subproblems, i.e., optimization of satellite clustering and beamforming. For the design of satellite clustering, the progress of satellite clustering is first formulated as a coalition formation game (CFG), which can cope with the frequent and rapid changes in the coalition of the satellite. Thereafter, a partial coalition preference order is proposed for determining the optimal satellite clustering and maximizing the sum rate. The results demonstrate that the proposed CFG converges to a stable exact potential game (EPG) with at least one Nash equilibrium (NE).

(3) An alternative method is proposed for optimizing the transceiver's beamforming and phase shifts of the satellite RIS. To elaborate, a zero forcing (ZF) precoder is first adopted to optimize the transmit precoder, thereby eliminating inter-user interference. Subsequently, the cyclic coordinate descent (CCD) optimization algorithm is proposed to determine the closed-form solution of the phase shift for

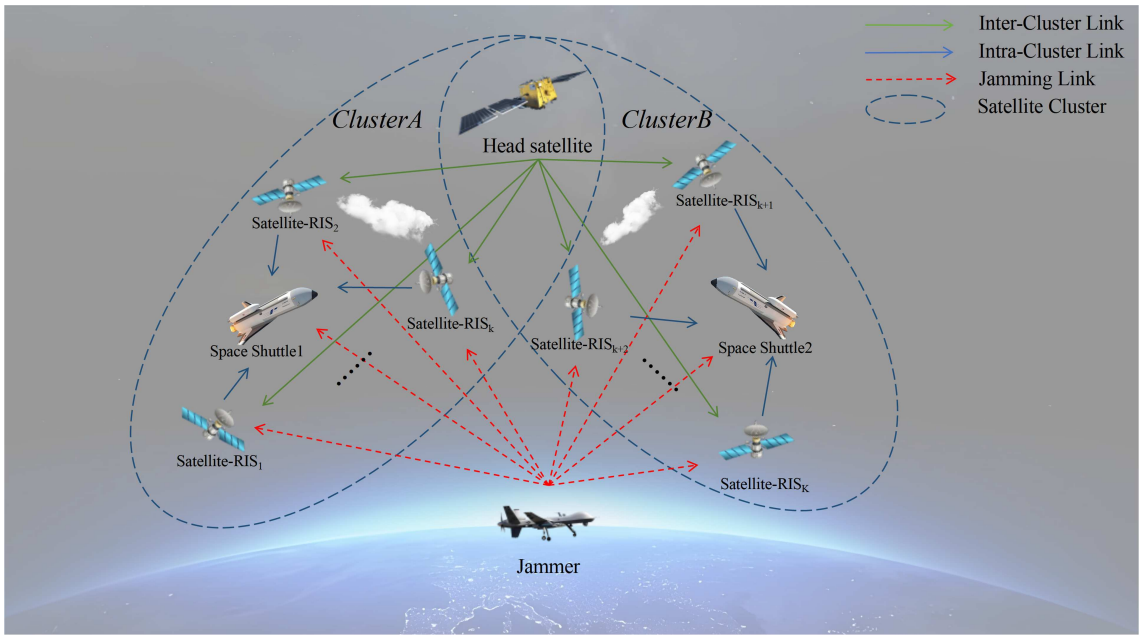

Figure 1 (Color online) Game-theoretic satellite clusters model.

multiple satellite RISs, leading to a significant decrease in computational complexity. Finally, the linear minimum-mean-square-error (MMSE) method is utilized to design the receive decoder. The simulation results clearly represent the effectiveness and superiority of the proposed schemes compared to existing approaches.

The layout of this paper is as follows. The system model and problem formulation are presented in Section 2. The proposed algorithm is presented in Section 3. Numerical results are provided in Section 4, and the conclusion is summarized in Section 5.

Notation. $\boldsymbol{X}^{\mathrm{H}}$, $\boldsymbol{X}^{\mathrm{T}}$, $\boldsymbol{X}^{*}$, and $\|\boldsymbol{X}\|_F$ denote the conjugate transpose, transpose, conjugate, and Frobenius norm of the matrix $\boldsymbol{X}$. The notations $\mathbb{E}\{\cdot\}$, $\mathrm{tr}\{\cdot\}$, $\Re\{\cdot\}$, $\Im\{\cdot\}$, and $\lambda\{\cdot\}$ denote the expectation, trace, real part, imaginary part, and eigenvalue of a complex number or matrix, respectively. $\mathbb{C}^{m\times n}$ represents the complex space of $m\times n$ dimensions. The symbol $\mathbb{H}^{n\times n}$ is the Hermitian matrix of $n\times n$ dimensions. $[\cdot]_{n,n}$ represents the n-th diagonal element of the matrix. The distribution of a circularly symmetric complex Gaussian random vector with a mean vector x and covariance matrix Σ is denoted by $\mathcal{CN}(x,\Sigma)$. diag is a diagonal matrix. $\mathcal{R}_{+}^{K}$ is the N-dimensional non-negative real domain.

2 System model and problem formulation

2.1 System model

As depicted in Figure 1, with the aid of n clustered satellite-RISs, a head satellite (HS, transmission satellite) with N_{L} antennas wishes to establish reliable links with k space shuttles. Meanwhile, a jammer utilizes a single omnidirectional antenna to impair the shuttles' signal reception from different angles. For simplicity of notion, the set of shuttles and satellite-RISs is denoted as $\mathcal{K}=\{1,2,\ldots,K\}$ and $\mathcal{N}=\{1,2,\ldots,N\}$, respectively. We assume that each shuttle and satellite-RIS are equipped with N_{U} antennas and N_{R} RIS units, respectively. The channel coefficients of the HS-RIS$_i$ link, the satellite-RIS$_i$-shuttle$_j$ link, the jammer-shuttle$_j$ link and the jammer-satellite-RIS$_i$ link are denoted by $\boldsymbol{H}_{\mathrm{HR}_i}\in\mathbb{C}^{N_{\mathrm{R}}\times N_{\mathrm{L}}}$, $\boldsymbol{H}_{\mathrm{R}_i\mathrm{U}_j}\in\mathbb{C}^{N_{\mathrm{U}}\times N_{\mathrm{R}}}$, $\boldsymbol{h}_{\mathrm{JU}_j}\in\mathbb{C}^{N_{\mathrm{U}}\times 1}$ and $\boldsymbol{h}_{\mathrm{JR}_i}\in\mathbb{C}^{N_{\mathrm{R}}\times 1}$ respectively, which follow the channel model in [40]. Moreover, we assume that the reflection coefficients of the i-th satellite-RIS is $\boldsymbol{p}_i=(p_1,\ldots,p_{\mathrm{N_R}})^{\mathrm{T}}$, where $p_i=\mathrm{e}^{\mathrm{j}\theta_i}$ and $\theta_i\in[0,2\pi]$. For ease of satellite, we denote the cascaded channels of HS-RIS$_i$-shuttle$_j$ link and jammer-RIS$_i$-shuttle$_j$ link as $\boldsymbol{H}_{\mathrm{HU}_{j,i}}=\boldsymbol{H}_{\mathrm{R}_i\mathrm{U}_j}\mathrm{diag}(\boldsymbol{p}_i)\boldsymbol{H}_{\mathrm{HR}_i}$ and $\boldsymbol{h}_{\mathrm{JU}_{j,i}}=\boldsymbol{H}_{\mathrm{R}_i\mathrm{U}_j}\mathrm{diag}(\boldsymbol{p}_i)\boldsymbol{h}_{\mathrm{JR}_i}$, respectively.

Denote $s_{\mathrm{T},j}$ as the symbol transmitted from HS to the j-th shuttle, where $\mathbb{E}[|s_{\mathrm{T},j}|^2]=1$. Prior to transmission, $s_{\mathrm{T},j}$ is weighted by the transmit beamforming vector $\boldsymbol{w}_{\mathrm{T},j}\in\mathbb{C}^{N_{\mathrm{L}}\times 1}$. As such, the

signal transmitted to the j-th shuttle can be represented as $\boldsymbol{x}_j = \boldsymbol{w}_{\mathrm{T},j} s_{\mathrm{T},j}$. Considering the HS's power constraint, the transmit must satisfy $\sum_{j=1}^{K} \|\boldsymbol{w}_{\mathrm{T},j}\|^2 \leqslant P_{\max}$, where $\|\cdot\|$ represents the Euclidean 2-norm, and $P_{\max}$ is the maximum transmit power. Furthermore, the receive beamforming vector of the j-th shuttle is $\boldsymbol{v}_j \in \mathbb{C}^{N_{\mathrm{U}} \times 1}$. Thus, the received signals at shuttle$_j$ is given by

$$\begin{aligned} y_j = &\sum_{i\in\mathcal{N}} \boldsymbol{v}_j^{\mathrm{H}} \boldsymbol{H}_{\mathrm{HU}_{j,i}} \boldsymbol{w}_{\mathrm{T},j} s_{\mathrm{T},j} + \sum_{k\neq j} \sum_{i\in\mathcal{N}} \boldsymbol{v}_j^{\mathrm{H}} \boldsymbol{H}_{\mathrm{HU}_{j,i}} \boldsymbol{w}_{T,k} s_{\mathrm{T},k} \\ &+ \sum_{i\in\mathcal{N}} \boldsymbol{v}_j^{\mathrm{H}} (\boldsymbol{h}_{\mathrm{JU}_{j,i}} + \boldsymbol{h}_{\mathrm{JU}_j}) \boldsymbol{w}_{\mathrm{J}} s_{\mathrm{J}} + \boldsymbol{v}_j^{\mathrm{H}} \boldsymbol{n}_j,\ \boldsymbol{n}_j \sim \mathcal{CN}(\boldsymbol{0}_{N_{\mathrm{U}}}, \sigma_j^2 \boldsymbol{I}_{N_{\mathrm{U}}}), \end{aligned} \tag{1}$$

where $\sigma_{\mathrm{U}_j}^2$ is the white noise power. Accordingly, the shuttle$_j$'s can be expressed as

$$\gamma_j = \frac{\left|\sum_{i\in\mathcal{N}} \boldsymbol{v}_j^{\mathrm{H}} \boldsymbol{H}_{\mathrm{HU}_{j,i}} \boldsymbol{w}_{\mathrm{T},j}\right|^2}{\left|\sum_{i\in\mathcal{N}} \boldsymbol{v}_j^{\mathrm{H}} \left(\boldsymbol{h}_{\mathrm{JU}_{j,i}} + \boldsymbol{h}_{\mathrm{JU}_j}\right) \boldsymbol{w}_{\mathrm{J}}\right|^2 + \left|\sum_{j\neq k} \sum_{i\in\mathcal{N}} \boldsymbol{v}_j^{\mathrm{H}} \boldsymbol{H}_{\mathrm{HU}_{j,i}} \boldsymbol{w}_{\mathrm{T},k}\right|^2 + \sigma_j^2}. \tag{2}$$

In view of the non-cooperative relationship between the communication party and the jammer, it is a challenge to get the accurate CSI of the jammer. As a result, this paper models the jammer's CSI uncertainty as a given continuous angle range [40], which can be expressed as

$$\Delta = \left\{\boldsymbol{h}_{\mathrm{JU}_j}, \boldsymbol{h}_{\mathrm{JR}_i} | \theta \in [\theta_L, \theta_U], \varphi \in [\varphi_L, \varphi_U], \forall j, i\right\}, \tag{3}$$

where θ, φ express the azimuth angle and elevation angle of the channels, respectively, (θ_L, θ_U) and (φ_L, φ_U) represent the bound of the corresponding angles.

It is worth noting that the transmission links in CCSAJ are modeled as quasi-static channels, ensuring that the temporal span of each transmission slot is confined within the channel coherence interval, thereby preserving time-selective channel stationarity. Consequently, the channel gain remains basically stationary in each transmission slot, but varies from different transmission slots [41].

2.2 Problem formulation

The objective of this paper is to improve transmission rate by jointly optimizing the satellite clustering, transceiver's beamforming, and satellite-RIS's phase shifts, under imperfect jammer's CSI. Accordingly, the problem can be modeled as

$$\begin{aligned} &\max_{\boldsymbol{w}_{\mathrm{T},j}, \boldsymbol{p}_i, \boldsymbol{v}_j, \mathrm{Co}_j} \min_{\Delta} \sum_{j\in\mathcal{K}} R[\mathrm{Co}_j], \\ &\text{s.t. } \mathrm{C1}: \sum_{j=1}^{K} \|\boldsymbol{w}_{\mathrm{T},j}\|^2 \leqslant P_{\max}, \quad \mathrm{C2}: \left|[\boldsymbol{p}_i]_{n,n}\right| = 1, \forall i, n, \\ &\quad \mathrm{C3}: \mathrm{Co}_j \subseteq \mathcal{N},\ \cup_{j\in\mathcal{K}} \mathrm{Co}_j = \mathcal{N},\ \mathrm{Co}_i \cap \mathrm{Co}_j = \varnothing, \forall i, j \in \mathcal{K}, i \neq j, \end{aligned} \tag{4}$$

where $R[\mathrm{Co}_j]$ is the sum rate of the cluster composed of the shuttle$_j$ and the serving satellite-RISs, i.e., $R[\mathrm{Co}_j] = \log_2(1 + \gamma_j)$, C1 is the transmitter power constraint, $P_{\max}$ is the maximum transmitter power; C2 is the satellite-RIS's phase shift matrix amplitude constraint; C3 is the clustering constraint.

3 Game-theoretic satellite clustering and scalable beamforming

In this section, we first divide the problem into two subproblems: satellite clustering optimization, transceiver's beamforming design and satellite-RIS's phase shifts design. Then, two efficient algorithms for solving two subproblems are proposed, which are detailed in the following.

3.1 Game-theoretic clustering

In order to solve the optimization problem of satellite clustering, we use CFG for networking, mainly because CFG has significant advantages in autonomy, flexibility, incentive mechanism, resource optimization, scalability and robustness. It is suitable for a complex network environment, can effectively

improve network performance and stability, and is suitable for the scenarios considered in this article. In addition, compared with the traditional networking algorithm, CFG can realize the composition of an ad-hoc network according to the order, so as to maximize the utilization of resources.

Definition 1 (CFG [42])**.** Each RIS can be arrenged into a nonoverlapping coalitions $\{\mathrm{Co}_j\}$, $\cup_{j\in\mathcal{K}}\mathrm{Co}_j = \mathcal{N}$, and each RIS has its own priority, which can be described as $\mathcal{P} = (\succ_1, \succ_2, \ldots, \succ_N)$, then the strategy $(\mathcal{N}, \mathcal{P})$ formulates CFG.

Each shuttle's utility function is defined as

$$u_i = R\left[\mathrm{Co}_j \cup n_i\right] - R\left[\mathrm{Co}_j\right],\ \forall n_i \notin \mathrm{Co}_j. \tag{5}$$

Actually, u_i is the extra gain with the participation of n_i.

The coalition preference order is the guide of the coalition change principle, which influences the action of coalition member. The above two aspects determine the performance of CFG. Then, we provide the details in the following.

(1) Coalition preference order. In CFG, whether coalition members are willing to change the coalition is determined by the coalition preference order, which includes selfish order, Pareto order, and equilibrium order [43, 44].

Definition 2 (Selfish order)**.** If the coalition member $n_i \in \mathrm{Co}_{j'}$ and the coalition formations $\{\mathrm{Co}_j, \mathrm{Co}_{j'}\}$, $j, j' \in \mathcal{K}$ satisfy (6), the selfish order in CFG is formed, i.e.,

$$\mathrm{Co}_j \succ_i \mathrm{Co}_{j'} \Leftrightarrow R\left[\mathrm{Co}_j \cup n_i\right] > R\left[\mathrm{Co}_{j'} \backslash n_i\right]. \tag{6}$$

Following the selfish order, each coalition member prioritizes enhancing the sum rate of the newly formed coalition, disregarding the performance of the current coalition.

Definition 3 (Pareto order)**.** If the coalition member $n_i \in \mathrm{Co}_{j'}$ and the coalition formations $\{\mathrm{Co}_j, \mathrm{Co}_{j'}\}$, $j, j' \in \mathcal{K}$ satisfy (7), the Pareto order in CFG is formed, i.e.,

$$\mathrm{Co}_j \succ_i \mathrm{Co}_{j'} \Leftrightarrow R\left[\mathrm{Co}_j \cup n_i\right] > R\left[\mathrm{Co}_j\right] \& R\left[\mathrm{Co}_{j'} \backslash n_i\right] > R\left[\mathrm{Co}_{j'}\right]. \tag{7}$$

Different from the selfish order, the Pareto order has better stability due to the strong constraints, which make coalition members cannot leave the current cluster easily. It is shown that the selfish order focuses on the utility of individual coalition member, while the Pareto order pays more attention to the overall system. To balance the utility of individual and that of overall system, we propose a equilibrium order.

Definition 4 (Equilibrium order)**.** If the coalition member $n_i \in \mathrm{Co}_{j'}$ and the coalition formations $\{\mathrm{Co}_j, \mathrm{Co}_{j'}\}$, $j, j' \in \mathcal{K}$ satisfy (8), the equilibrium order in CFG is formed, i.e.,

$$\begin{aligned} \mathrm{Co}_j \succ_i \mathrm{Co}_{j'} &\Leftrightarrow u_i\left(\mathrm{Co}_j \cup n_i\right) > u_i\left(\mathrm{Co}_{j'}\right) \\ &\Leftrightarrow R\left[\mathrm{Co}_j \cup n_i\right] - R\left[\mathrm{Co}_j\right] > R\left[\mathrm{Co}_{j'}\right] - R\left[\mathrm{Co}_{j'} \backslash n_i\right] \\ &\Leftrightarrow R\left[\mathrm{Co}_j \cup n_i\right] + R\left[\mathrm{Co}_{j'} \backslash n_i\right] > R\left[\mathrm{Co}_j\right] + R\left[\mathrm{Co}_{j'}\right]. \end{aligned} \tag{8}$$

According to the equilibrium order, the coalition change of each coalition member will further improve the sum rate of both the target and current coalition, i.e., Co_j and $\mathrm{Co}_{j'}$, as well as the performance of the overall system.

(2) Coalition change principle. In this paper, we adopt the affiliation principle as the coalition change principle based on the proposed equilibrium order.

Definition 5 (Affiliation principle)**.** The coalition member n_i chooses to leave the current coalition $\mathrm{Co}_{j'}$ and enter the target coalition Co_j, if and only if the system get better sum rate according to the equilibrium order, namely,

$$n_i \to \mathrm{Co}_j \Leftrightarrow u_i\left(\mathrm{Co}_j \cup n_i\right) > u_i\left(\mathrm{Co}_{j'}\right), \forall \mathrm{Co}_j, \mathrm{Co}_{j'}\ \ \forall n_i \in \mathrm{Co}_{j'}. \tag{9}$$

Algorithm 1 Game-theoretic clustering algorithm.

input: The set of satellite-RISs $\mathcal{N}$ and shuttles $\mathcal{K}$.
Initialize: Each satellite-RIS selects a shuttle to provide communication assistance randomly.
loop
  Randomly select a satellite-RIS n_i and calculate its current coalition formation utility $u_i(\mathrm{Co}_{j'})$;
  The selected satellite-RIS n_i choose another shuttle $j \in \mathcal{K}, j \neq j'$ for access and evaluate the explored utility $u_i\left(\mathrm{Co}_j\right)$;
  if $u_i\left(\mathrm{Co}_j\right) > u_i\left(\mathrm{Co}_{j'}\right)$ is satisfied **then**
    The satellite-RIS changes its current coalition and take part in the target one: $\mathrm{Co}_{j'} \to \mathrm{Co}_{j'} \backslash n_i, \mathrm{Co}_j \to \mathrm{Co}_j \cup n_i$;
  end if
end loop: All the satellite-RISs do not change their coalitions;
output: Stable coalition formation $\{\mathrm{Co}_j\}^*$.

Definition 6 (Stable coalition formation)**.** If any coalition member cannot improve the utility by changing its current coalition selection, the coalition formation is stable, which is given by

$$u_i\left(\mathrm{Co}_j, \mathrm{Co}_{-j}\right) \geqslant u_i\left(\mathrm{Co}_{j'}, \mathrm{Co}_{-j'}\right), \forall n_i \in \mathcal{N}, \quad \mathrm{Co}_j, \mathrm{Co}_{j'} \in \left\{\cup_{j=1}^{k} \mathrm{Co}_j\right\}. \tag{10}$$

Theorem 1. If equilibrium order is adopted as the coalition preference order, the proposed CFG can converge to a stable coalition formation.

Proof. EPG is employed to verify that a CFG with equilibrium order can reach a stable coalition formulation, which is defined as follows.

Definition 7 (EPG [44])**.** If there is a potential function that satisfies (11), the game can be regarded as an EPG with at least one NE point:

$$\varphi(\mathrm{Co}_j, \mathrm{Co}_{-j}) - \varphi(\mathrm{Co}_{j'}, \mathrm{Co}_{-j'}) = u_i(\mathrm{Co}_j) - u_i(\mathrm{Co}_{j'}), \tag{11}$$

where Co_{-j} denotes the coalition without n_i.

We assumed the sum rate of the system as the potential function, i.e., $\varphi(\mathrm{Co}_j, \mathrm{Co}_{-j}) = R_{\mathrm{sum}} = \sum_{j \in \mathcal{K}} R[\mathrm{Co}_j]$. When the coalition selection of satellite-RIS n_i changes from $\mathrm{Co}_{j'}$ to Co_j, the increase of potential function can be express as

$$\begin{aligned} \varphi(\mathrm{Co}_j, \mathrm{Co}_{-j}) - \varphi(\mathrm{Co}_{j'}, \mathrm{Co}_{-j'}) =& R[\mathrm{Co}_j \cup n_i] + R[\mathrm{Co}_{j'} \backslash n_i] \\ &+ R[\{\cup_{j \in \mathcal{K}} \mathrm{Co}_j\} \backslash \{\mathrm{Co}_j \cup n_i\} \backslash \{\mathrm{Co}_{j'} \backslash n_i\}] \\ &- R[\mathrm{Co}_j] - R[\mathrm{Co}_{j'}] - R[\{\cup_{j \in \mathcal{K}} \mathrm{Co}_j\} \backslash \mathrm{Co}_j \backslash \mathrm{Co}_{j'}]. \end{aligned} \tag{12}$$

Since the change of the node's coalition strategy only impacts the achievable rate of the current coalition and the target coalition, which does not impact other coalitions, as such, we have

$$R[\{\cup_{j \in k} \mathrm{Co}_j\} \backslash \{\mathrm{Co}_j \cup n_i\} \backslash \{\mathrm{Co}_{j'} \backslash n_i\}] = R[\{\cup_{j \in k} \mathrm{Co}_j\} \backslash \mathrm{Co}_j \backslash \mathrm{Co}_{j'}]. \tag{13}$$

Combining (12) and (13), the increase of potential function can be further expressed as

$$\begin{aligned} \varphi(\mathrm{Co}_j, \mathrm{Co}_{-j}) - \varphi(\mathrm{Co}_{j'}, \mathrm{Co}_{-j'}) &= R[\mathrm{Co}_j \cup n_i] + R[\mathrm{Co}_{j'} \backslash n_i] - R[\mathrm{Co}_j] - R[\mathrm{Co}_{j'}] \\ &= R[\mathrm{Co}_j \cup n_i] - R[\mathrm{Co}_j] - (R[\mathrm{Co}_{j'}] - R[\mathrm{Co}_{j'} \backslash n_i]) \\ &= u_i(\mathrm{Co}_j) - u_i(\mathrm{Co}_{j'}). \end{aligned} \tag{14}$$

Observed from (11) and (14) can be found that the increase of the potential function and the coalition formation utility are equal. Thus, the CFG with equilibrium order is an EPG with at least one NE. Specifically, the potential function will increase when each satellite-RIS changes its coalition to improve the utility function. Moreover, due to the finite number of users and satellite-RISs, the possible results of coalition formulation are limited. After enough iterations, the coalition formulation with the highest potential function will be achieved. There must exist at least one coalition formulation to improve the utility if the final coalition formation $\{\mathrm{Co}_j\}^*$ is erratic. Finally, the stable coalition formulation is formed and the NE point is achieved. Theorem 1 is proved.

Finally, we provide the detailed game-theoretic clustering algorithm in Algorithm 1.

3.2 Scalable beamforming

After optimizing satellite clustering via CFG, we focus on designing the beamforming. Due to the imperfect jammer's CSI, we obtain robust CSI by discretizing the uncertainty region Δ, and then applying the alternating optimization method to decouple and optimize multiple beamforming variables.

3.2.1 *Discretization method for CSI uncertainty*

To transform the intractable optimization problem in (4) with Δ into a solvable one, we adopt the discretization method in [45] to address Δ. In elaborate, Δ is discretized into a set of S ($S>1$) samples, i.e.,

$$\tilde{\Delta}=\left\{\boldsymbol{h}_{\mathrm{JU}_{j,1}},\ldots,\boldsymbol{h}_{\mathrm{JU}_{j,S}},\boldsymbol{h}_{\mathrm{JR}_{i,1}},\ldots,\boldsymbol{h}_{\mathrm{JR}_{i,S}}\right\}. \tag{15}$$

It is worth noting that as $S\to\infty$, discretizing $\tilde{\Delta}$ approximates the continuity of Δ. Furthermore, the azimuth angle and elevation angle inside Δ are uniformly discretized, namely

$$\begin{aligned}&\theta^{(p)}=\theta_L+(k-1)\Delta\theta, k=1,\ldots,Q_1,\\&\varphi^{(q)}=\varphi_L+(m-1)\Delta\varphi, m=1,\ldots,Q_2,\end{aligned} \tag{16}$$

where $\theta^{(k)}$ and $\varphi^{(m)}$ represent the azimuth angle and elevation angle of channel $\boldsymbol{h}_{\mathrm{JU}_j}^{(k,m)}$ and $\boldsymbol{h}_{\mathrm{JR}_i}^{(k,m)}$, respectively, $\Delta\theta=\frac{\theta_U-\theta_L}{Q_1-1}$, and $\Delta\varphi=\frac{\varphi_U-\varphi_L}{Q_2-1}$. Thus, we can obtain the robust jammer's CSI $\tilde{\boldsymbol{h}}_{\mathrm{JU}_j}=\sum_{k=1}^{Q_1}\sum_{m=1}^{Q_2}(\frac{1}{Q_1Q_2})\boldsymbol{h}_{\mathrm{JU}_j}^{(k,m)}$ and $\tilde{\boldsymbol{h}}_{\mathrm{JR}_i}=\sum_{k=1}^{Q_1}\sum_{m=1}^{Q_2}(\frac{1}{Q_1Q_2})\boldsymbol{h}_{\mathrm{JR}_i}^{(k,m)}$. By substituting the robust jammer's CSI into problem (4), Δ can be removed. Therefore, the optimization problem can be reformulated as

$$\begin{aligned}\max_{\boldsymbol{w}_{\mathrm{T},j},\boldsymbol{P}_i,\boldsymbol{v}_j}\ &\sum_{j\in\mathcal{K}}\log_2\left(1+\frac{\left|\sum_{i\in\mathcal{N}}\boldsymbol{v}_j^{\mathrm{H}}\boldsymbol{H}_{\mathrm{HU}_{j,i}}\boldsymbol{w}_{\mathrm{T},j}\right|^2}{\left|\sum_{i\in\mathcal{N}}\boldsymbol{v}_j^{\mathrm{H}}\left(\boldsymbol{h}_{\mathrm{JU}_{j,i}}+\boldsymbol{h}_{\mathrm{JU}_j}\right)\boldsymbol{w}_{\mathrm{J}}\right|^2+\left|\sum_{j\neq k}\sum_{i\in\mathcal{N}}\boldsymbol{v}_j^{\mathrm{H}}\boldsymbol{H}_{\mathrm{HU}_{j,i}}\boldsymbol{w}_{\mathrm{T},k}\right|^2+\sigma_j^2}\right),\\&\text{s.t. C1}:\sum_{j=1}^{K}\|\boldsymbol{w}_{\mathrm{T},j}\|^2\leqslant P_{\max},\quad \text{C2}:\left|[\boldsymbol{P}_i]_{n,n}\right|=1,\forall i,n,\end{aligned} \tag{17}$$

where C1 is the transmitter power constraint, $P_{\max}$ is the maximum transmission power; C2 is the amplitude constraint of the RIS's phase shift matrix.

3.2.2 *Beamforming design*

First, we turn to optimizing the transmit beamforming $\boldsymbol{w}_{\mathrm{T},j}$. Considering the system is a multi-user MIMO system, the ZF algorithm in [46] is the optimal solution for $\boldsymbol{w}_{\mathrm{T},j}$. Specifically, the ZF algorithm transmits the signals towards the intended targets with nulls steered in the direction of other users, whose ZF matrix is

$$\boldsymbol{W}^{\bigstar}=\beta_{\mathrm{ZF}}\boldsymbol{G}\left(\boldsymbol{G}^{\mathrm{H}}\boldsymbol{G}\right)^{-1}, \tag{18}$$

where $\beta_{\mathrm{ZF}}=\sqrt{P_{\max}/\mathrm{tr}((\boldsymbol{G}^{\mathrm{H}}\boldsymbol{G})^{-1})}$, $\boldsymbol{G}_j^{\mathrm{H}}=\boldsymbol{v}_j^{\mathrm{H}}(\sum_{i\in\mathrm{Co}_j}\boldsymbol{H}_{\mathrm{R}_i\mathrm{U}_j}\mathrm{diag}(\boldsymbol{p}_i)\boldsymbol{H}_{\mathrm{LR}_i})$, and $\boldsymbol{G}_j^{\mathrm{H}}$ is the k-th column of $\boldsymbol{G}$. Here, $\boldsymbol{W}^{\bigstar}=[\boldsymbol{w}_{\mathrm{T}_1}^{\bigstar},\ldots,\boldsymbol{w}_{\mathrm{T}_\mathrm{K}}^{\bigstar}]$, each column of which represents the transmit beamforming for the k-th shuttle.

After adopting the ZF algorithm to eliminate the inter-user interference, the beamforming subproblem can be reduced to a sum rate maximization problem within one cluster, i.e.,

$$\begin{aligned}\max_{\boldsymbol{p}_i,\boldsymbol{v}_j}\ &\log_2\left(1+\frac{\left|\sum_{i\in\mathrm{Co}_j}\boldsymbol{v}_j^{\mathrm{H}}\boldsymbol{H}_{\mathrm{LU}_{j,i}}\boldsymbol{w}_{\mathrm{T},j}\right|^2}{\left|\sum_{i\in\mathrm{Co}_j}\boldsymbol{v}_j^{\mathrm{H}}(\boldsymbol{h}_{\mathrm{JU}_{j,i}}+\boldsymbol{h}_{\mathrm{JU}_j})\boldsymbol{w}_{\mathrm{J}}\right|^2+\sigma^2}\right),\\&\text{s.t. C2}:\left|[\boldsymbol{p}_i]_{n,n}\right|=1,\forall i,n.\end{aligned} \tag{19}$$

Due to the monotonicity of the logarithmic function, the objective function of (19) can also be reformulated as

$$\max_{\boldsymbol{p}_i,\boldsymbol{v}_j}\ \gamma=\frac{\left|\sum_{i\in\mathrm{Co}_j}\boldsymbol{v}_j^{\mathrm{H}}\boldsymbol{H}_{\mathrm{LU}_{j,i}}\boldsymbol{w}_{\mathrm{T},j}\right|^2}{\left|\sum_{i\in\mathrm{Co}_j}\boldsymbol{v}_j^{\mathrm{H}}(\boldsymbol{h}_{\mathrm{JU}_{j,i}}+\boldsymbol{h}_{\mathrm{JU}_j})\boldsymbol{w}_{\mathrm{J}}\right|^2+\sigma^2},$$

$$\text{s.t. C2}: \left|[\boldsymbol{p}_i]_{n,n}\right| = 1, \forall i, n. \tag{20}$$

Define $\boldsymbol{u}_{1,i}^{\mathrm{H}} = \boldsymbol{v}_j^{\mathrm{H}} \boldsymbol{H}_{\mathrm{R}_i\mathrm{U}} \mathrm{diag}(\boldsymbol{H}_{\mathrm{LR}_i} \boldsymbol{w}_{\mathrm{T},j})$, $\boldsymbol{u}_{2,i}^{\mathrm{H}} = \boldsymbol{v}_j^{\mathrm{H}} \boldsymbol{H}_{\mathrm{R}_i\mathrm{U}} \mathrm{diag}(\boldsymbol{h}_{\mathrm{JR}_i} \boldsymbol{w}_{\mathrm{J}})$ and $\hat{\boldsymbol{p}}_j = [\boldsymbol{p}_1, \ldots, \boldsymbol{p}_i]$, $i \in \mathrm{Co}_j$ as intermediate variables. Removing the constant term in (20), the subproblem for optimizing the RIS's phase shifts is recast as

$$\begin{aligned} &\max_{\hat{\boldsymbol{p}}_j} \ \gamma = \frac{\left|\hat{\boldsymbol{u}}_1^{\mathrm{H}} \hat{\boldsymbol{p}}_j\right|^2}{\left|h_{\mathrm{J}} + \hat{\boldsymbol{u}}_2^{\mathrm{H}} \hat{\boldsymbol{p}}_j\right|^2 + \sigma^2}, \\ &\text{s.t. C2}: \left|[\hat{\boldsymbol{p}}_j]_{n,n}\right| = 1, \ \forall n, \end{aligned} \tag{21}$$

where $\hat{\boldsymbol{u}}_1^{\mathrm{H}} \hat{\boldsymbol{p}}_j = \sum_{i \in \mathrm{Co}_j} \boldsymbol{u}_{1,i}^{\mathrm{H}} \boldsymbol{p}_i$, $\hat{\boldsymbol{u}}_2^{\mathrm{H}} \hat{\boldsymbol{p}}_j = \sum_{i \in \mathrm{Co}_j} \boldsymbol{u}_{2,i}^{\mathrm{H}} \boldsymbol{p}_i$, $h_{\mathrm{J}} = \sqrt{P_{\mathrm{J}}} \boldsymbol{v}^{\mathrm{H}} \boldsymbol{h}_{\mathrm{JU}}$. However, the objective function is a non-convex quadratic fractional function, which prevents us from solving it. To address this issue, the Dinkelbach method is adopted to convert the objective function of (21) into the following equivalent form, i.e.,

$$\hat{\boldsymbol{p}}_j^{\mathrm{H}} \hat{\boldsymbol{U}}_1 \hat{\boldsymbol{p}}_j - \eta \left(|h_{\mathrm{J}}|^2 + 2\Re \left(h_{\mathrm{J}} \hat{\boldsymbol{u}}_2^{\mathrm{H}} \hat{\boldsymbol{p}}_j \right) + \hat{\boldsymbol{p}}_j^{\mathrm{H}} \hat{\boldsymbol{U}}_2 \hat{\boldsymbol{p}}_j + \sigma^2 \right), \tag{22}$$

where η is a non-negative Dinkelbach parameter, $\hat{\boldsymbol{U}}_1 = \hat{\boldsymbol{u}}_1 \hat{\boldsymbol{u}}_1^{\mathrm{H}}$, $\hat{\boldsymbol{U}}_2 = \hat{\boldsymbol{u}}_2 \hat{\boldsymbol{u}}_2^{\mathrm{H}}$, $\boldsymbol{U} = \hat{\boldsymbol{U}}_1 - \eta \hat{\boldsymbol{U}}_2$, $\tilde{\boldsymbol{u}}_2^{\mathrm{H}} = \eta h_{\mathrm{J}} \hat{\boldsymbol{u}}_2^{\mathrm{H}}$. As such, we can obtain the optimization subproblem for $\hat{\boldsymbol{p}}_j$, namely

$$\begin{aligned} &\max_{\hat{\boldsymbol{p}}_j} \hat{\boldsymbol{p}}_j^{\mathrm{H}} \hat{\boldsymbol{U}} \hat{\boldsymbol{p}}_j - 2\Re \left(\tilde{\boldsymbol{u}}_2^{\mathrm{H}} \hat{\boldsymbol{p}}_j \right), \\ &\text{s.t. C2:} \left|[\hat{\boldsymbol{p}}_j]_{n,n}\right| = 1, \forall n. \end{aligned} \tag{23}$$

Then, we employ the CCD algorithm to solve it, which involves constructing a new vector $[\eta; \hat{\boldsymbol{p}}_j]$ with $\hat{N}_{\mathrm{R},j} + 1$ variables, where $\hat{N}_{\mathrm{R},j} = \sum_{i \in \mathrm{Co}_j} N_{\mathrm{R},i}$. Specifically, we first expand the objective function of the equation, which is given by

$$\begin{aligned} \tilde{\boldsymbol{p}}_j^{\mathrm{H}} \hat{\boldsymbol{U}} \tilde{\boldsymbol{p}}_j - 2\Re \left(\tilde{\boldsymbol{u}}_2^{\mathrm{H}} \tilde{\boldsymbol{p}}_j \right) &= \sum_{k=1}^{\hat{N}_{\mathrm{R},j}} \sum_{i=1}^{\hat{N}_{\mathrm{R},j}} \tilde{p}_{j,i}^* \hat{\boldsymbol{U}}_{(i,k)} \tilde{p}_{j,k} - 2\Re \left(\sum_{i=1}^{\hat{N}_{\mathrm{R},j}} \tilde{u}_{2,i}^* \tilde{p}_{j,k} \right) \\ &= \sum_{i=1}^{\hat{N}_{\mathrm{R},j}} \tilde{p}_{j,i}^* \hat{\boldsymbol{U}}_{(i,i)} \tilde{p}_{j,i} + \sum_{k \neq i}^{\hat{N}_{\mathrm{R},j}} \sum_{i=1}^{\hat{N}_{\mathrm{R},j}} \tilde{p}_{j,i}^* \hat{\boldsymbol{U}}_{(i,k)} \tilde{p}_{j,k} - 2\Re \left(\sum_{i=1}^{\hat{N}_{\mathrm{R},j}} \tilde{u}_{2,i}^* \tilde{p}_{j,k} \right) \\ &= \sum_{i=1}^{\hat{N}_{\mathrm{R},j}} \hat{\boldsymbol{U}}_{(i,i)} + \Re \left\{ \sum_{i=1}^{\hat{N}_{\mathrm{R},j}} \tilde{p}_{j,i}^* \left(\hat{\boldsymbol{U}}_{(i)} - 2\tilde{u}_{2,i} \right) \right\}, \end{aligned} \tag{24}$$

where $\hat{\boldsymbol{U}}_{(i)} = \sum_{k=1}^{k<i} \hat{\boldsymbol{U}}_{(i,k)} \tilde{p}_{j,k} + \sum_{k>i}^{\hat{N}_{\mathrm{R},j}} \hat{\boldsymbol{U}}_{(i,k)} \tilde{p}_{j,k}$. Armed with (24), a subproblem involving $\hat{N}_{\mathrm{R},j} + 1$ variables can be obtained, and we update the above variables by using the CCD algorithm, which is expressed as

$$\begin{cases} \eta^{(i_d+1)} = \dfrac{\left|\hat{c}_1^{\mathrm{H}} \tilde{\boldsymbol{p}}_j^{(i_d)}\right|^2}{\left|h_J + \hat{c}_2^{\mathrm{H}} \tilde{\boldsymbol{p}}_j^{(i_d)}\right|^2 + \sigma_{\mathrm{U}}^2}, \\ \tilde{p}_{j,1}^{(i_d+1)} = \underset{\tilde{p}_{j,1} \in \mathcal{A}}{\arg\max}\, e \left(\eta^{(i_d+1)}, \tilde{p}_{j,1}, \tilde{p}_{j,2}^{(i_d)}, \ldots, \tilde{p}_{j,\hat{N}_{\mathrm{R},j}}^{(i_d)} \right), \\ \qquad \vdots \\ \tilde{p}_{j,i}^{(i_d+1)} = \underset{\tilde{p}_{j,i} \in \mathcal{A}}{\arg\max}\, e \left(\eta^{(i_d+1)}, \tilde{p}_{j,1}^{(i_d+1)}, \ldots, \tilde{p}_{j,i-1}^{(i_d+1)}, \tilde{p}_{j,i}, \tilde{p}_{j,i+1}^{(i_d)}, \ldots, \tilde{p}_{j,\hat{N}_{\mathrm{R},j}}^{(i_d)} \right), \\ \qquad \vdots \\ \tilde{p}_{j,\hat{N}_{\mathrm{R},j}}^{(i_d+1)} = \underset{\tilde{p}_{j,\hat{N}_{\mathrm{R},j}} \in \mathcal{A}}{\arg\max}\, e \left(\eta^{(i_d+1)}, \tilde{p}_{j,1}^{(i_d+1)}, \tilde{p}_{j,2}^{(i_d+1)}, \ldots, \tilde{p}_{j,\hat{N}_{\mathrm{R},j}-1}^{(i_d+1)}, \tilde{p}_{j,\hat{N}_{\mathrm{R},j}} \right), \end{cases} \tag{25}$$

Algorithm 2 Proposed CFG-BF optimization algorithm.

input: The set of RISs $\mathcal{N}$ and shuttles $\mathcal{K}$ and the CSI of jamming channel.
Initialize: Set the iteration index $t=0$. Generate the initial beams $\{\{\boldsymbol{w}_{\mathrm{T},j}\}^{(0)},\{\boldsymbol{p}_i\}^{(0)},\{\boldsymbol{v}_j\}^{(0)}\}$ and the initial coalition $\{\mathrm{Co}_j\}^{(0)}$;
repeat
  For given $\{\{\boldsymbol{w}_{\mathrm{T},j}\}^{(t)},\{\boldsymbol{p}_i\}^{(t)},\{\boldsymbol{v}_j\}^{(t)}\}$, update $\{\mathrm{Co}_j\}^{(t)}$ to $\{\mathrm{Co}_j\}^{(t+1)}$ through Algorithm 1;
  if coalition formation $\{\mathrm{Co}_j\}$ changed **then**
    Optimize $\{\boldsymbol{w}_{\mathrm{T},j}\}^{(t)}$ to $\{\boldsymbol{w}_{\mathrm{T},j}\}^{(t+1)}$ with ZF algorithm based on the new coalition $\{\mathrm{Co}_j\}^{(t+1)}$ and $\{\{\boldsymbol{p}_i\}^{(t)},\{\boldsymbol{v}_j\}^{(t)}\}$;
    Optimize $\{\boldsymbol{p}_i\}^{(t)}$ to $\{\boldsymbol{p}_i\}^{(t+1)}$ with CCD algorithm based on the new coalition $\{\mathrm{Co}_j\}^{(t+1)}$ and $\{\{\boldsymbol{w}_{\mathrm{T},j}\}^{(t+1)},\{\boldsymbol{v}_j\}^{(t)}\}$;
    Optimize $\{\boldsymbol{v}_j\}^{(t)}$ to $\{\boldsymbol{v}_j\}^{(t+1)}$ with MMSE algorithm based on the new coalition $\{\mathrm{Co}_j\}^{(t+1)}$ and $\{\{\boldsymbol{w}_{\mathrm{T},j}\}^{(t+1)},\{\boldsymbol{p}_i\}^{(t+1)}\}$;
  end if
  $t=t+1$;
until The coalition formulation is stable or $t=t_{\max}$;
output: Optimal cooperative coalition formation $\{\mathrm{Co}_j\}^{*}$ and scalable beamforming vector $\{\{\boldsymbol{w}_{\mathrm{T},j}\}^{(*)},\{\boldsymbol{p}_i\}^{(*)},\{\boldsymbol{v}_j\}^{(*)}\}$.

where $\mathcal{A}=\{|z|=1\,|z\in\mathbb{C}\}$, $e\left(\cdot\right)=\Re\{\sum_{i=1}^{\hat{N}_{\mathrm{R},j}}\tilde{p}_{j,i}^{*}(\hat{\boldsymbol{U}}_{(i)}-2\tilde{u}_{2,i})\}$. As for each optimization variable, the optimization subproblem can be formulated as

$$\begin{aligned}&\max_{\tilde{p}_{j,i}}\Re\left\{\tilde{p}_{j,i}^{*}\left(\sum_{k=1}^{k<i}\hat{\boldsymbol{U}}_{(i,k)}\tilde{p}_{j,k}^{(i_d+1)}+\sum_{k>i}^{\hat{N}_{\mathrm{R},j}}\hat{\boldsymbol{U}}_{(i,k)}\tilde{p}_{j,k}^{(i_d)}-2\tilde{u}_{2,i}\right)\right\},\\&\text{s.t. C2:}\,|\tilde{p}_{j,i}|=1,\forall i.\end{aligned}\tag{26}$$

Obviously, the optimal closed-form solution for the expression can be obtained, i.e.,

$$\tilde{p}_{j,i}^{\bigstar}=\exp\left\{j\arg\left(\sum_{k=1}^{k<i}\hat{\boldsymbol{U}}_{(i,k)}\tilde{p}_{j,k}^{(i_d+1)}+\sum_{k>i}^{\hat{N}_{\mathrm{R},j}}\hat{\boldsymbol{U}}_{(i,k)}\tilde{p}_{j,k}^{(i_d)}-2\tilde{u}_{2,i}\right)\right\}.\tag{27}$$

Alternately updating η and $\tilde{\boldsymbol{p}}_j$, we can get the optimal closed-form solution for RIS's phase shifts.

Finally, we optimize the receive decoder $\boldsymbol{v}_j$. According to [47], the linear MMSE decoder can be adopted to solve the problem. Thus, we can obtain the optimal closed-form solution for $\boldsymbol{v}$, whose expression is as below

$$\boldsymbol{v}_j^{\bigstar}=\frac{\left(\bar{\boldsymbol{w}}_{\mathrm{T},j}\bar{\boldsymbol{w}}_{\mathrm{T},j}^{\mathrm{H}}+P_{\mathrm{J}}\bar{\boldsymbol{w}}_{\mathrm{J}}\bar{\boldsymbol{w}}_{\mathrm{J}}^{\mathrm{H}}+\sigma_{\mathrm{U}}^{2}\boldsymbol{I}_{\hat{N}_{\mathrm{R}}}\right)^{\dagger}\bar{\boldsymbol{w}}_{\mathrm{T},j}}{\left\|\left(\bar{\boldsymbol{w}}_{\mathrm{T},j}\bar{\boldsymbol{w}}_{\mathrm{T},j}^{\mathrm{H}}+P_{\mathrm{J}}\bar{\boldsymbol{w}}_{\mathrm{J}}\bar{\boldsymbol{w}}_{\mathrm{J}}^{\mathrm{H}}+\sigma_{\mathrm{U}}^{2}\boldsymbol{I}_{\hat{N}_{\mathrm{R}}}\right)^{\dagger}\bar{\boldsymbol{w}}_{\mathrm{T},j}\right\|},\tag{28}$$

where $\bar{\boldsymbol{w}}_{\mathrm{T},j}=\sum_{i=1}^{n}\boldsymbol{H}_{\mathrm{R}_i\mathrm{U}_j}\mathrm{diag}(\boldsymbol{p}_i)\boldsymbol{H}_{\mathrm{HR}_i}\boldsymbol{w}_{\mathrm{T},j}$, $\bar{\boldsymbol{w}}_{\mathrm{J}}=\left(\boldsymbol{h}_{\mathrm{J}}+\sum_{i=1}^{n}\boldsymbol{H}_{\mathrm{R}_i\mathrm{U}_j}\mathrm{diag}(\boldsymbol{p}_i)\boldsymbol{h}_{\mathrm{JR}_i}\right)$.

3.3 Convergence and complexity analysis

We summarize the proposed CFG-BF algorithm in Algorithm 2 for a better understanding. Then, we prove the convergence of the proposed algorithm, which includes two parts, i.e., the game-theoretic clustering and the beamforming design. As stated in Theorem 1, the game-theoretic clustering tends to a stable coalition formation. Thus, this subsection proves the convergence of the beamforming design, which mainly depends on the CCD. The ascent of (22) can be expressed as

$$\begin{aligned}e\left(\eta^{(id)},\tilde{p}_{j,1}^{(id)},\tilde{p}_{j,2}^{(id)},\ldots,\tilde{p}_{j,\hat{N}_R}^{(id)}\right)&\overset{a}{\leqslant}e\left(\eta^{(id)},\tilde{p}_{j,1}^{(id+1)},\tilde{p}_{j,2}^{(id)},\ldots,\tilde{p}_{j,\hat{N}_{\mathrm{R},j}}^{(id)}\right)\\&\overset{b}{\leqslant}e\left(\eta^{(id+1)},\tilde{p}_{j,1}^{(id+1)},\tilde{p}_{j,2}^{(id)},\ldots,\tilde{p}_{j,\hat{N}_{\mathrm{R},j}}^{(id)}\right)\\&\overset{a}{\leqslant}e\left(\eta^{(id+1)},\tilde{p}_{j,1}^{(id+1)},\tilde{p}_{j,2}^{(id+1)},\ldots,\tilde{p}_{j,\hat{N}_{\mathrm{R},j}}^{(id)}\right)\\&\overset{b}{\leqslant}e\left(\eta^{(id+2)},\tilde{p}_{j,1}^{(id+1)},\tilde{p}_{j,2}^{(id+1)},\ldots,\tilde{p}_{j,\hat{N}_{\mathrm{R},j}}^{(id)}\right)\\&\vdots\\&\overset{a}{\leqslant}e\left(\eta^{(id+\hat{N}_{\mathrm{R},j}-1)},\tilde{p}_{j,1}^{(id+1)},\tilde{p}_{j,2}^{(id+1)},\ldots,\tilde{p}_{j,\hat{N}_{\mathrm{R},j}}^{(id+1)}\right)\end{aligned}$$

$$\overset{b}{\leqslant} e\left(\eta^{(id+\hat{N}_{\mathrm{R},j})}, \tilde{p}_{j,1}^{(id+1)}, \tilde{p}_{j,2}^{(id+1)}, \ldots, \tilde{p}_{j,\hat{N}_{\mathrm{R},j}}^{(id+1)}\right). \tag{29}$$

The inequality a holds from the fact that $\tilde{p}_{j,i}^{(id)}$ is a unique element-wise maximize of $e\left(\eta, \tilde{\boldsymbol{p}}_j\right)$, which will be given next. The inequality b holds based on [48].

To further prove the proposed algorithm's convergence, we discuss the uniqueness of the element-wise maximizer of $\hat{p}_{j,i}$. Recalling the solution (27) of problem (26), namely, $\hat{p}_{j,i} = \exp\{j \arg(\tilde{\boldsymbol{U}}_{(i)})\}$, where $\tilde{\boldsymbol{U}}_{(i)} = \sum_{k=1}^{k<i} \hat{\boldsymbol{U}}_{(i,k)} \tilde{p}_{j,k}^{(i_d+1)} + \sum_{k>i}^{\hat{N}_{\mathrm{R},j}} \hat{\boldsymbol{U}}_{(i,k)} \tilde{p}_{j,k}^{(i_d)} - 2\tilde{c}_{2,i}$, we can show that Eq. (27) is the unique element-wise maximizer by contradiction. Denoting $\bar{p}_{j,i} = \exp\{j \arg(\tilde{\boldsymbol{U}}_{(i)} + \theta_i)\}$ as anther element-wise maximizer, where θ_i is not an integer multiple of 2π, we have

$$\begin{aligned} e\left(\eta, \tilde{\boldsymbol{p}}_j\right) &= \sum_{i=1}^{\hat{N}_{\mathrm{R},j}} \hat{\boldsymbol{U}}_{(i,i)} + \sum_{i=1}^{\hat{N}_{\mathrm{R},j}} \left|\tilde{\boldsymbol{U}}_{(i)}\right|, \\ e\left(\eta, \bar{\boldsymbol{p}}_j\right) &= \sum_{i=1}^{\hat{N}_{\mathrm{R},j}} \hat{\boldsymbol{U}}_{(i,i)} + \sum_{i=1}^{\hat{N}_{\mathrm{R},j}} \left|\tilde{\boldsymbol{U}}_{(i)}\right| \cos\left(\theta_i\right). \end{aligned} \tag{30}$$

Since both $\tilde{\boldsymbol{p}}_j$ and $\bar{\boldsymbol{p}}_j$ maximize $e(\eta, \tilde{\boldsymbol{p}}_j)$, we obtain $e(\eta, \tilde{\boldsymbol{p}}_j) = e(\eta, \bar{\boldsymbol{p}}_j)$ so that θ_i must be an integer multiple of 2π, which contradicts our assumption. Thus, Eq. (27) is the unique element-wise maximizer of $e(\eta, \tilde{\boldsymbol{p}}_j)$, such that inequality b holds, which implies that the sequence $\{\eta^{(id)}, \tilde{\boldsymbol{p}}_j^{(id)}\}$ is monotonically increasing. Furthermore, the objective function $\{\eta^{(id)}, \tilde{\boldsymbol{p}}_j^{(id)}\}$ is upper-bounded by the constraint C2. Hence, $\{\eta^{(id)}, \tilde{\boldsymbol{p}}_j^{(id)}\}$ increases to the limited point $\{\eta^{\infty}, \tilde{\boldsymbol{p}}_j^{\infty}\}$. Thus, the proposed beamforming algorithm converges to the optimal solution. Combining the convergence of game-theoretic clustering and the beamforming design, the overall algorithm can converge to the fixed solution.

Then, we will prove the scalability of the proposed algorithm compared to existing algorithms by calculating its complexity. Specifically, the complexity of the proposed algorithm mainly includes three parts: satellite clustering based on CFG, CCD algorithm for (23) and optimization of $\boldsymbol{w}_{\mathrm{T},j}$ and $\boldsymbol{v}_j$. We donate I_1 and ε as the total number of alternating optimization algorithm's number and the fault tolerance of the CCD algorithm, respectively. According to [49], the complexity of updating a single $\tilde{p}_i$ in (25) is $\mathcal{O}(\hat{N}_{\mathrm{R},j})$, and the complexity of CCD algorithm in (23) could be described as $\mathcal{O}[(\frac{1}{\varepsilon^2})(\hat{N}_{\mathrm{R},j}^2 + 1)]$. Next, we can get the complexity of optimizing $\boldsymbol{w}_{\mathrm{T},j}$ and $\boldsymbol{v}_j$ is $\mathcal{O}(N_{\mathrm{U}}\hat{N}_{\mathrm{R},j})$ and $\mathcal{O}(N_{\mathrm{T}}\hat{N}_{\mathrm{R},j})$ based on [7]. As such, the complexity of the alternating optimization algorithm can be expressed as

$$\mathcal{O}_{\mathrm{AO}} = I_1 \left[\mathcal{O}\left[\left(\frac{1}{\varepsilon^2}\right)\left(\hat{N}_{\mathrm{R},j}^2 + 1\right)\right] + \mathcal{O}\left(N_{\mathrm{U}}\hat{N}_{\mathrm{R},j}\right) + \mathcal{O}\left(N_{\mathrm{T}}\hat{N}_{\mathrm{R},j}\right)\right]. \tag{31}$$

The proposed game-theoretic clustering algorithm involves the comparison between the current coalition and new coalition and the update for possible coalition switch where complexity can be represented as $\mathcal{O}\left(\mathcal{U}_1\right)$ and $\mathcal{O}\left(\mathcal{U}_2\right)$, respectively. We donate I_2 as the number of convergence iteration, and the complexity of CFG-based cohesive satellite clustering can be described as $I_2\left[\mathcal{O}\left(\mathcal{U}_1\right) + \mathcal{O}\left(\mathcal{U}_2\right)\right]$. Thus, the total complexity could be expressed in the following form:

$$\mathcal{O}_{\mathrm{CCSAJ}} = I_1 \left[\mathcal{O}\left[\left(\frac{1}{\varepsilon^2}\right)\left(\hat{N}_{\mathrm{R},j}^2 + 1\right)\right] + \mathcal{O}\left(N_{\mathrm{U}}\hat{N}_{\mathrm{R},j}\right) + \mathcal{O}\left(N_{\mathrm{T}}\hat{N}_{\mathrm{R},j}\right)\right] + I_2\left[\mathcal{O}\left(\mathcal{U}_1\right) + \mathcal{O}\left(\mathcal{U}_2\right)\right]. \tag{32}$$

For the SCA algorithm, due to the optimization problem with $\hat{N}_{\mathrm{R}} + 3$ optimization variables and $\hat{N}_{\mathrm{R}}$ constraints in cvx. The complexity of SCA algorithm is $\mathcal{O}[(\frac{1}{\varepsilon^2})\hat{N}_{\mathrm{R}}(\hat{N}_{\mathrm{R},j} + 2)^2]$. Compared with the complexity of the CCD algorithm, the proposed algorithm has better scalability.

4 Simulation and results

In this section, the performance of the proposed algorithm is demonstrated and verified through numerical simulation. The simulation parameters are summarized in Table 1. In this study, the jamming pattern of the hostile jammer is set to fixed power and frequency jamming, and the jamming power is set to

Table 1 Simulation parameters.

Parameter	Symbol	Value
RIS number	n	6
Shuttle number	k	2
Transmission power	$P_{\max}$	10 W
Bandwidth	B	10 MHz
Noise power	σ^2	10^{-11}
Multi-path number	N_m	5
Jamming channel uncertainty	Δ	6°

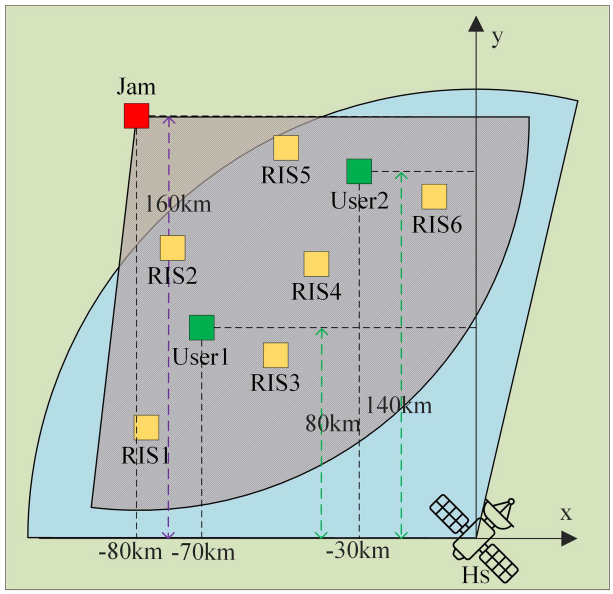

Figure 2 (Color online) Simulation scenario.

10 W, which is simplified. The RISs and shuttles are randomly deployed in the task area, as shown in Figure 2. Additionally, the path-loss factor g_d follows a complex Gaussian distribution with a mean of 0 and a variance of $10^{\frac{\mathrm{PL}}{10}}$, where $g_d \sim \mathcal{CN}(0, 10^{\frac{\mathrm{PL}}{10}})$, $\mathrm{PL} = -30.18 - 26 \lg d_s$ and d_s is the link distance. The channel model from [40] was adopted to model the jamming channel and legitimate channel. The communication scenarios and methods for comparing the simulation are summarized in the table below.

(1) Proposed algorithm. In this scenario, the equilibrium order is chosen as the coalition preference order. The CFG method is used to optimize the clustering, after which the CCD method is used to optimize the phase shift matrix of the RIS.

(2) Selfish order. In this scenario, the selfish order is chosen as the coalition preference order. The deployment method and the optimized algorithm in this scenario are consistent with those of the previous scenario.

(3) Pareto order. In this scenario, the Pareto order is chosen as the coalition preference order. The deployment method and the optimized algorithm in this scenario are consistent with those of the first scenario.

(4) Perfect CSI. In this scenario, the CSI of the imperfect jammer is replaced by the perfect CSI.

(5) SCA algorithm. In this scenario, the coalition preference order is the equilibrium order. The deployment method in this scenario is consistent with that of the previous scenario.

(6) Random clustering. In this scenario, the CFG is no longer used to form clusters. Instead, the RISs are randomly deployed and provided to the shuttle. The other components of the scenario remain unchanged.

(7) Single RIS. In this scenario, only a single intelligent surface, RIS_1, is retained.

Figure 3 presents the distribution of the satellite RISs and the shuttles using the proposed algorithm in the presence of a jammer. Using the proposed algorithm, the coalition is obtained for each RIS in a distributed way. Figure 3(a) shows the expected condition for satellite clustering, while Figure 3(b)

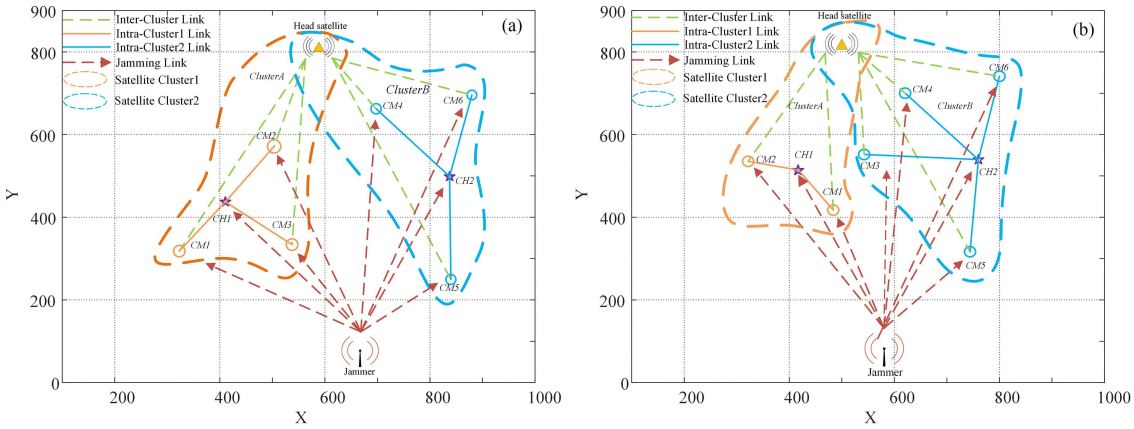

Figure 3 (Color online) (a) Coalition formation for cohesive clustered satellites under ideal conditions; (b) coalition formation for cohesive clustered satellites with overlapping areas.

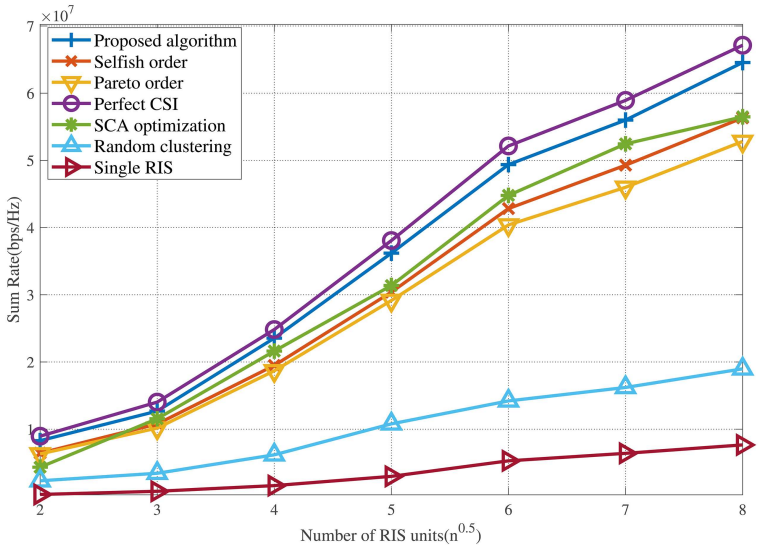

Figure 4 (Color online) Comparison of sum rate of different benchmark schemes and scenarios with different numbers of RIS.

shows the condition where some of the RISs are deployed in overlapping areas. The proposed algorithm could achieve effective clustering under both conditions.

Figure 4 presents a comparison of the performance of the proposed algorithm using different coalition preference orders, beamforming optimization algorithms, and scenarios with different numbers of RIS units. Due to the nonlinear growth of the number of RIS units during the simulation, in order to facilitate analysis and visualization, the value obtained by taking the square root of the number of units is taken as the abscissa in Figure 4. The performance of the proposed algorithm is far superior to that achieved with random clustering. Moreover, the sum rate increases with the number of RIS units because the topology based on game-theoretic clustering efficiently utilizes resources by dynamically adjusting the structure of the satellite. Additionally, the proposed order can achieve better performance compared to the other two orders. The selfish order tends to improve the individual utility when choosing a new coalition, which considers the utility of other coalitions while improving its own utility. In contrast, due to the stringent constraints on the performance of the current coalition and the new coalition, the Pareto order achieves a lower sum rate compared with the equilibrium order. Moreover, for the single RIS with the CCD algorithm, the system performance is significantly lower than that of the proposed algorithm because, in the single RIS scenario, the jammer's channel is positively correlated with the communication channel when there is a jammer. By improving the reflection matrix optimization, the strength of both the received signal and the jammer's signal will be enhanced, resulting in a sharp decline in the communication performance. The simulation result also demonstrates the superior anti-jamming

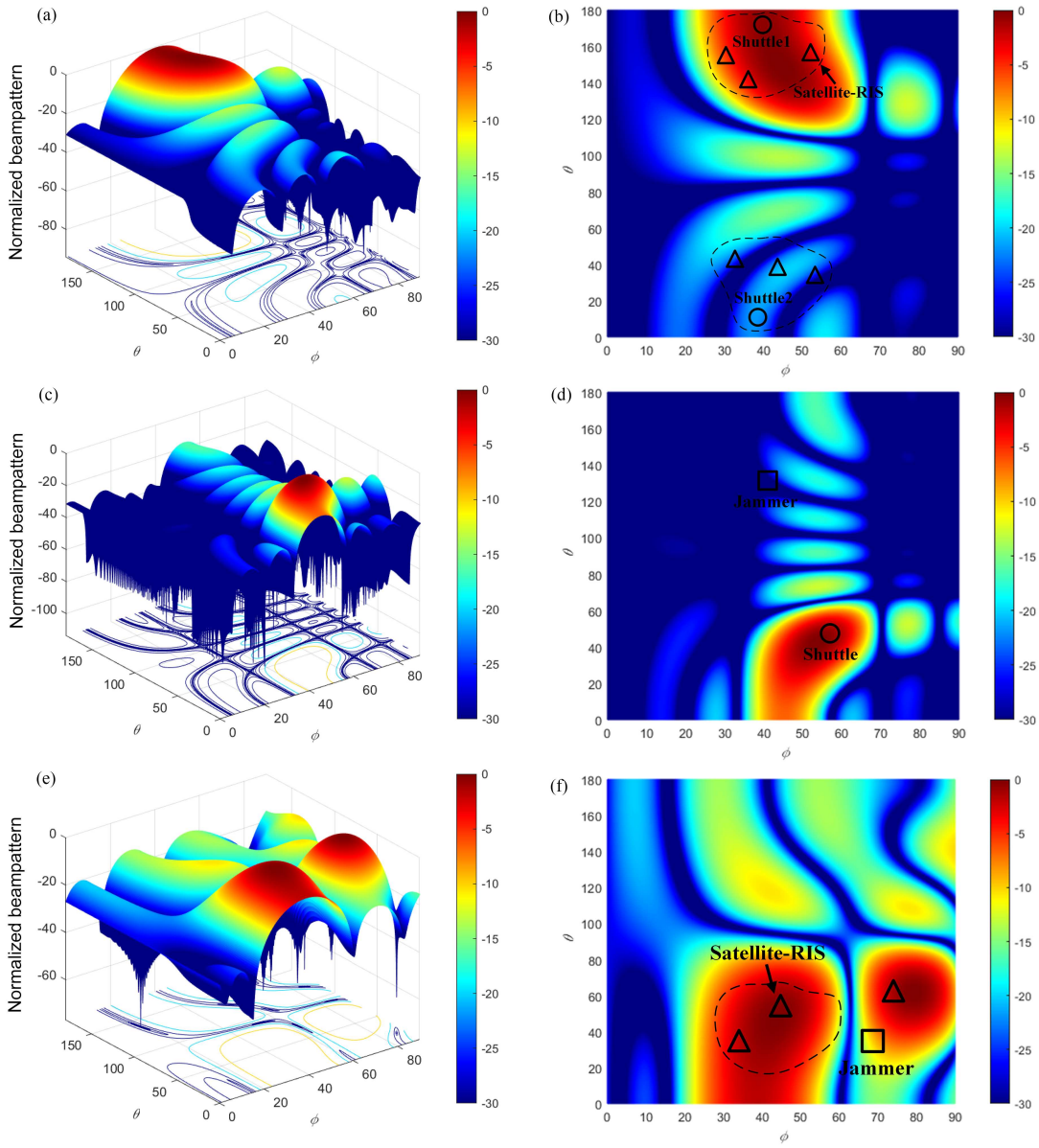

Figure 5 (Color online) (a) 3D and (b) 2D Tx beam pattern of $\boldsymbol{w}_{\mathrm{T},1}$; (c) 3D and (d) 2D reflecting beam pattern of $\boldsymbol{p}_2$; (e) 3D and (f) 2D Rx beam pattern of $\boldsymbol{v}_1$.

performance of the proposed algorithm compared to that of the SCA algorithm.

Figure 5 illustrates the partially optimized radiation beam patterns of the Co_1. Here, the main focus is on investigating the Tx beam pattern of HS and the Rx beam pattern of $\mathrm{shuttle}_1$, as well as the reflecting beam pattern of the single satellite RIS. The optimized mainlobe of HS clearly points in the region of the target area and simultaneously aligns the nulls toward undesired targets. The beam pattern of the RIS achieved the same performance, the sum rate increased, and the anti-jamming performance was improved. Thus, the proposed game-theoretic clustering and scalable beamforming method can effectively improve the security of transmission and anti-jamming performance under the condition that the jammer's CSI is imperfect.

Figure 6 shows the sum rate of the proposed method for different channel uncertainties, where the data verify the impact of different jamming environments. Here, factors such as the jamming power and location of deployment of the jammer can affect the signal reception of the receiver. Therefore, the comprehensive effect of various jamming factors was considered to verify the performance of the algorithm, namely, the uncertainty of the jamming channel. The performance of all methods remained almost unchanged as the channel uncertainty increased. Robust processing of the imperfect CSI is not

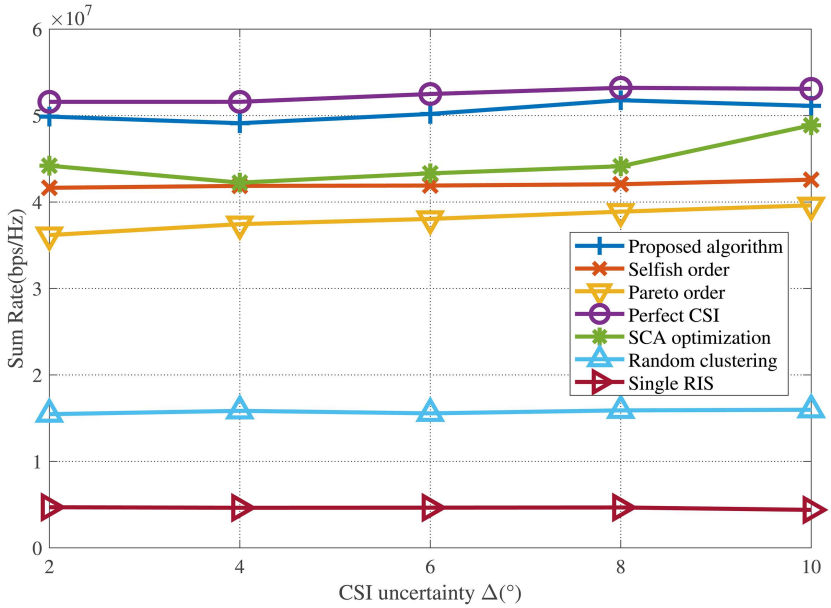

Figure 6 (Color online) Comparison of the sum rate of different benchmark schemes and scenarios with differences in the CSI uncertainty.

only applicable to the method proposed in this study but also to other methods and can effectively reduce the impact of CSI uncertainty.

5 Conclusion

A novel multi-RIS-assisted CCSAJ framework was established to defend against jamming attacks. In a scenario where the jammer's CSI is imperfect, a worst-case optimization problem was formulated to maximize the sum rate by jointly optimizing the satellite clustering, transceiver's beamforming, and phase shifts of the satellite RIS. In particular, the progress of satellite clustering was formulated as a CFG, and the equilibrium order for obtaining the optimal satellite clustering and maximizing the sum rate was proposed. The results prove that the proposed CFG can converge to a stable EPG with at least one NE. An alternative optimization method was also proposed for optimizing the transceiver's beamforming and phase shifts of the satellite RIS. The proposed algorithm has a certain degree of scalability, which is manifested in the following aspects. (1) The CFG can dynamically adjust policies based on the coalition preference order, achieving self-organization of the network. (2) The CCD algorithm reduces the computational complexity, making it applicable to larger-scale scenarios. (3) The modular design enables the system to adapt to constantly changing scenarios. The results of the numerical simulation demonstrate the superiority and validity of the proposed schemes over existing benchmark schemes.

References

1 Jiao J, Wu S, Lu R, et al. Massive access in space-based internet of things: challenges, opportunities, and future directions. IEEE Wireless Commun, 2021, 28: 118–125
2 He Y, Sheng B, Yin H, et al. Multi-objective deep reinforcement learning based time-frequency resource allocation for multi-beam satellite communications. China Commun, 2022, 19: 77–91
3 Chen W Y, Ding H Y, Wang S L, et al. Beamforming design for covert broadcast communication with hidden adversary. Sci China Inf Sci, 2024, 67: 162304
4 He Y, Xiao Y, Zhang S, et al. Direct-to-smartphone for 6G NTN: technical routes, challenges, and key technologies. IEEE Netw, 2024, 38: 128–135
5 Jung D H, Im G, Ryu J G, et al. Satellite clustering for non-terrestrial networks: concept, architectures, and applications. IEEE Veh Technol Mag, 2023, 18: 29–37
6 He Y, Liu Y, Jiang C, et al. Multiobjective anti-collision for massive access ranging in MF-TDMA satellite communication system. IEEE Int Things J, 2022, 9: 14655–14666
7 Yang Z, Chen M, Saad W, et al. Energy-efficient wireless communications with distributed reconfigurable intelligent surfaces. IEEE Trans Wireless Commun, 2022, 21: 665–679
8 Jiao J, Liao S Y, Sun Y Y, et al. Fairness-improved and QoS-guaranteed resource allocation for NOMA-based S-IoT network. Sci China Inf Sci, 2021, 64: 169306
9 Jiao J, Yang P, Du Z, et al. Clustered multi-criteria routing algorithm for mega low Earth orbit satellite constellations. IEEE Trans Veh Technol, 2024, 73: 13790–13803
10 Xu L, Jiao J, Jiang S Y, et al. Semantic-aware coordinated transmission in cohesive clustered satellites: utility of information perspective. Sci China Inf Sci, 2024, 67: 199301

11 Liu J, Wang F, Tang X, et al. A multipath error cancellation method based on antenna jitter. Commun Eng, 2025, 4: 17
12 Lin X, Liu A J, Han C, et al. Intelligent adaptive MIMO transmission for nonstationary communication environment: a deep reinforcement learning approach. IEEE Trans Commun, 2025. doi: 10.1109/TCOMM.2025.3529263
13 Ouyang M, Zhang R, Wang B, et al. Network coding-based multipath transmission for LEO satellite networks with domain cluster. IEEE Int Things J, 2024, 11: 21659–21673
14 Liu Q, Li X, Ji H, et al, Multi-path routing algorithm with joint optimization of load-balancing for cluster-based LEO satellite networks. In: Proceedings of the 8th IEEE International Conference on Network Intelligence and Digital Content (IC-NIDC), Beijing, 2023. 264–268
15 Jung S, Bang E, Hwang Y, et al. Modeling of inter-satellite link protocol for satellite constellation. In: Proceedings of the 14th International Conference on Information and Communication Technology Convergence (ICTC), Jeju, 2023. 1612–1613
16 Yang Z, Long F, Sun F, et al, A novel routing algorithm based on dynamic clustering for LEO satellite networks. In: Proceedings of the IEEE Pacific Rim Conference on Communications, Computers and Signal Processing, Victoria, 2011. 145–148
17 Lu R, Lu R M. An anti-jamming improvement strategy for satellite frequency-hopping communication. In: Proceedings of the International Conference on Wireless Communications and Signal Processing, Nanjing, 2009. 1–5
18 Lee D, Kim D S, Lim C M, et al. Performance analysis of frequency hopping satellite communication system reducing the transient response of polyphase DFT filter. In: Proceedings of the 20th Asia-Pacific Conference on Communication (APCC2014), Pattaya, 2014. 199–202
19 Barton R J. Distributed MIMO communication using small satellite constellations. In: Proceedings of the IEEE International Conference on Wireless for Space and Extreme Environments (WiSEE), Noordwijk, 2014. 1–7
20 van Chien T, Tu L T, Chatzinotas S, et al. Coverage probability and ergodic capacity of intelligent reflecting surface-enhanced communication systems. IEEE Commun Lett, 2021, 25: 69–73
21 Sun Y, Zhu Y, An K, et al. Active-passive cascaded RIS-aided receiver design for jamming nulling and signal enhancing. IEEE Trans Wireless Commun, 2024, 23: 5345–5362
22 Sun Y, An K, Yu M, et al. Dual-polarized stacked metasurface transceiver design with rate splitting for next-generation wireless networks. IEEE J Sel Areas Commun, 2025, 43: 811–833
23 He R, Li G, Chen J, et al. Joint power and beamformer optimization in multi-antenna relay covert system: exploiting public users as shelter. IEEE Trans Wireless Commun, 2025, 24: 385–400
24 Mei W, Zhang R. Joint base station and IRS deployment for enhancing network coverage: a graph-based modeling and optimization approach. IEEE Trans Wireless Commun, 2023, 22: 8200–8213
25 Fu M, Mei W, Zhang R. Multi-active/passive-IRS enabled wireless information and power transfer: active IRS deployment and performance analysis. IEEE Commun Lett, 2023, 27: 2217–2221
26 Mei W, Zhang R. Cooperative beam routing for multi-IRS aided communication. IEEE Wireless Commun Lett, 2021, 10: 426–430
27 Cui M, Zhang G, Zhang R. Secure wireless communication via intelligent reflecting surface. IEEE Wireless Commun Lett, 2019, 8: 1410–1414
28 Mei W, Zhang R. Multi-IRS deployment optimization for enhanced wireless coverage: a performance-cost trade-off. In: Proceedings of the IEEE International Conference on Communications (ICC), Rome, 2023. 2056–2061
29 Mei W, Wang D, Chen Z, et al. Joint beam routing and resource allocation optimization for multi-IRS-reflection wireless power transfer. IEEE Trans Wireless Commun, 2024, 23: 16606–16620
30 Wang L, Zhou T, Xu T, et al. Sum rate maximization for multi-IRS assisted downlink NOMA with mobile users. In: Proceedings of the IEEE International Conference on Communications (ICC), Seoul, 2022. 3778–3783
31 Tekbiyik K, Kurt G K, Yanikomeroglu H. Energy-efficient RIS-assisted satellites for IoT networks. IEEE Int Things J, 2022, 9: 14891–14899
32 Xu S, Liu J, Cao Y, et al. Intelligent reflecting surface enabled secure cooperative transmission for satellite-terrestrial integrated networks. IEEE Trans Veh Technol, 2021, 70: 2007–2011
33 Xiao X, You L, Wang K Z, et al. Distortion-aware beamforming design for multi-beam satellite communications with nonlinear power amplifiers. Sci China Inf Sci, 2024, 67: 162302
34 Cao X, Yang B, Huang C, et al. Converged reconfigurable intelligent surface and mobile edge computing for space information networks. IEEE Netw, 2021, 35: 42–48
35 Sun Y, Lin Z, An K, et al. Multi-functional RIS-assisted semantic anti-jamming communication and computing in integrated aerial-ground networks. IEEE J Sel Areas Commun, 2024, 42: 3597–3617
36 Sun Y, An K, Zhu Y, et al. Energy-efficient hybrid beamforming for multilayer RIS-assisted secure integrated terrestrial-aerial networks. IEEE Trans Commun, 2022, 70: 4189–4210
37 An K, Sun Y, Lin Z, et al. Exploiting multi-layer refracting RIS-assisted receiver for HAP-SWIPT networks. IEEE Trans Wireless Commun, 2024, 23: 12638–12657
38 Yang H, Liu S, Xiao L, et al. Learning-based reliable and secure transmission for UAV-RIS-assisted communication systems. IEEE Trans Wireless Commun, 2024, 23: 6954–6967
39 Yang H, Lin K, Xiao L, et al. Energy harvesting UAV-RIS-assisted maritime communications based on deep reinforcement learning against jamming. IEEE Trans Wireless Commun, 2024, 23: 9854–9868
40 Sun Y, An K, Luo J, et al. Intelligent reflecting surface enhanced secure transmission against both jamming and eavesdropping attacks. IEEE Trans Veh Technol, 2021, 70: 11017–11022
41 Lin X, Liu A, Ni W, et al. Sum rate maximization of ad-hoc network in adversarial communication environments: a game-theoretic approach. IEEE Trans Veh Technol, 2024, 73: 17905–17910
42 Qi N, Huang Z, Sun W, et al. Coalitional formation-based group-buying for UAV-enabled data collection: an auction game approach. IEEE Trans Mobile Comput, 2023, 22: 7420–7437
43 Qi N, Huang Z, Zhou F, et al. A task-driven sequential overlapping coalition formation game for resource allocation in heterogeneous UAV networks. IEEE Trans Mobile Comput, 2023, 22: 4439–4455
44 Gao Z, Liu A, Xu X, et al. Sum data minimization in LEO satellite-UAV integrated multi-tier computing networks: a game-theoretic multiple access approach. IEEE Trans Commun, 2024, 72: 1701–1715
45 Sun Y, An K, Zhu Y, et al. RIS-assisted robust hybrid beamforming against simultaneous jamming and eavesdropping attacks. IEEE Trans Wireless Commun, 2022, 21: 9212–9231
46 Ragunathan S, Dananjayan S, Perumal D, et al. Energy efficiency in multicell massive MIMO network using zero forcing technique. In: Proceedings of the IEEE International Conference on System, Computation, Automation and Networking (ICSCA), Pondicherry, 2018. 1–4
47 Wong V, Schober R, Ng D W K, et al. Key Technologies for 5G Wireless Systems. Cambridge: Cambridge University Press, 2017
48 Shen K, Yu W. Fractional programming for communication systems—part I: power control and beamforming. IEEE Trans Signal Process, 2018, 66: 2616–2630
49 Arora A, Tsinos C G, Shankar M R B, et al. Efficient algorithms for constant-modulus analog beamforming. IEEE Trans Signal Process, 2022, 70: 756–771